

## Examples of principles behind the industrial metallic products

Dr. Yoshiharu Mae

### Abstract

Not recognized in general but in fact, theories and what we could call *principles* are often hidden behind the industrial products.

Here three examples of such kind are introduced.

The first one shows the relationship between mechanical properties, crystallographic orientation and manufacturing conditions. The second one shows the way of applying the characteristics of intermetallic compound to the real product. The third one shows the way of applying the electrochemistry to the real product.

### Introduction

In the textbook on materials science of the Open University in England, it is stated that “*engineers often deny the use of the abstract sciences that they have (probably) all studied*”. [1]

This seems to be a common phenomenon throughout the world.

For example, a retired Japanese steel engineer said in the following:

When he graduated from the university, entered the steel company and was delivered to the steel making factory as a freshman in 1956, he was told by a predecessor that what he learned

at the university was useless, therefore he should see the facts and think by himself. But he was deeply impressed by discovering that the real huge 60 ton furnace behaved according to the textbook which he learned at the university against the words of the predecessor. [2]

From my experiences also, I was often surprised at the deep theories during the development of the metallic products. Here I would like to introduce the examples of such experiences. The first one is the example in which production itself was not possible without knowing the principles and second two are the examples in which production was possible but for the improvement the clarification of principles was necessary.

### 1 Development of manufacturing process of titanium alloy sheet

(The relationship between mechanical properties, crystallographic orientation and manufacturing conditions)

Titanium is a 4A group metal at the 4<sup>th</sup> cycle in the periodic table. Titanium has a density of 4.5 g/cm<sup>3</sup>, 40% lighter than iron and has the high strength, therefore it is used in the aircraft. But it is very hard to fabricate titanium alloys due to their strong chemical activity, hexagonal crystal structure of high anisotropy, high strength, low Young's modulus and low thermal conductivity etc..

Fig. 1 shows the titanium alloy product produced by forging for the aircraft.

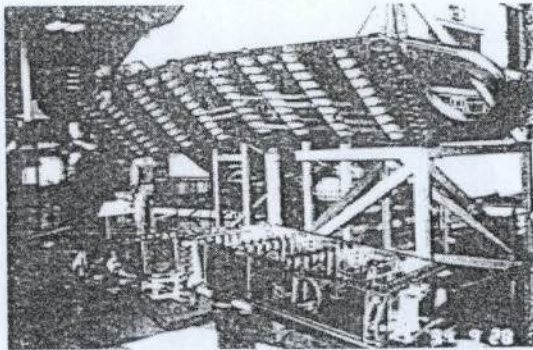


Fig.1 Titanium alloy product for aircraft

In the aircraft, sheets of thickness around 1mm are also used.

But manufacturing titanium alloy sheets is very difficult because of the high strength, high yield strength to tensile strength ratio, low ductility, low Young's modulus etc..

Moreover, an unexpected difficulty is the control of crystallographic orientation (texture) during manufacturing processes.

In titanium alloy (Ti-6Al-4V) sheet, only minimum bending radius and minimum yield and tensile strength are specified. But in practice, it is hard to satisfy these properties.

If we make titanium alloy sheet by rolling without appropriate knowledge, we get the sheet with the crystallographic orientation shown in Fig. 2.

Fig. 2 shows the pole figure of the crystallographic orientation of such a sheet and the schematic presentation of such crystallographic orientation (bad orientation).

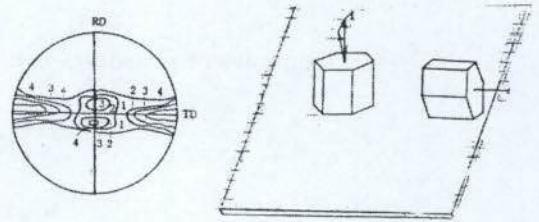


Fig. 2 Pole figure and schematic orientation of titanium hexagonal crystals in Ti-6Al-4V alloy sheet (bad orientation)

Sheets with this texture have low yield strength and inferior bendability in the rolling direction in spite of the large elongation in the tensile test. It appears strange that bendability (formability) is bad in the direction with good elongation (ductility).

But it can not be said that bendability is proportional to the elongation. It is because that bending undergoes plane strain condition. Fig.3 shows the strain condition at bending of the sheet.

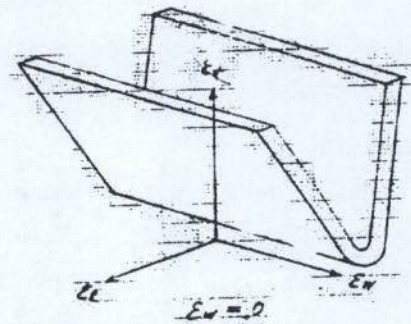


Fig. 3 Strain condition at bending

At bending, elongation strain in the perpendicular direction to the bending axis must be compensated by the shrinkage strain in the thickness direction because the deformation in the transverse direction is constrained.

Here the property that the strain in the thickness direction is likely to occur is questioned.



Such a property is expressed by r- value. R-value is defined as is shown in Fig.4.

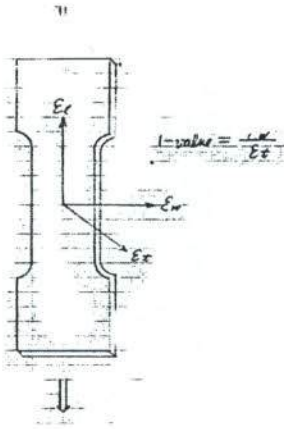


Fig. 4 Definition of r-value

In general, for instance, at steel sheet etc., r-value is maintained above 1 in order to resist the thinning of the thickness during deep drawing. But at bending, high r-value is harmful. The titanium sheets with the texture shown in Fig. 2 have very large r-values over 2 or 3. In order to lower r-values, crystallographic orientation (texture) must be changed. In conclusion, good crystallographic orientation which satisfies the strength and bendability is one as is shown in Fig. 5.

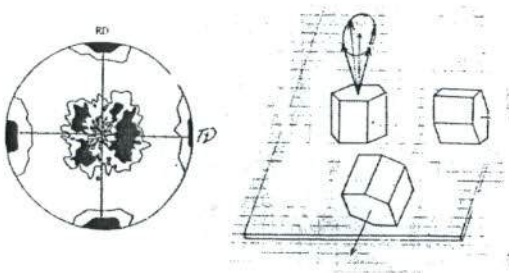


Fig. 5 Pole figure and schematic orientation of titanium hexagonal crystals in Ti-6Al-4V alloy sheet (good orientation)

Omitting the details of research and saying only the result, such a texture is obtained through the following mechanism.[3]

First, (110)[011] texture is formed during rolling in the β-phase-rich temperature range, which is typical in b.c.c. metals.

Second, as the β-phase transforms into α-phase during cooling after rolling, the orientation of β-phase changes to that of α-phase according to Burgers relationship. I.e.,

$$(0001)_{hcp} \parallel \{011\}_{bcc}$$

$$[1\bar{1}\bar{1}]_{hcp} \parallel \langle 111 \rangle_{bcc}$$

This orientation relationship is shown in fig. 6.

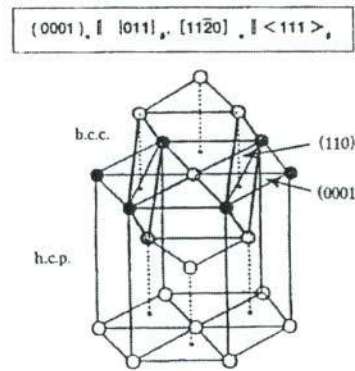


Fig. 6 Burgers orientation relationship

The positions of (001) poles of (001)[011] texture are shown in Fig. 7.

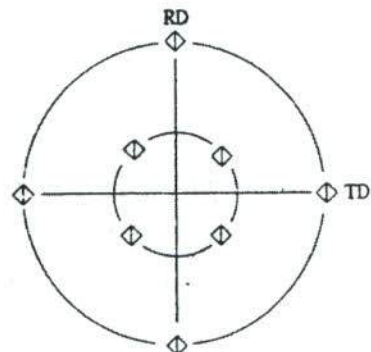


Fig. 7 The positions of (001) poles of (001)[011] texture

According to Burgers orientation relationship, the positions of (001) poles of  $\beta$ -phase directly become those of (0002) poles of  $\alpha$ -phase. This coincides well with the pole figure in Fig. 5. In practice, the sheets with this type of texture have low  $r$ -values (nearly 1) and high yield strength and good bendability.

Commercial sheets with this type of texture are being produced by special ways.

But sometimes sheets with various  $r$ -values are shipped to markets, especially in case of  $\alpha$ -phase titanium alloy sheets such as Ti-5Al-2.5Sn alloy. Fig. 8 shows the effect of  $r$ -values on the Erichsen-value and Fig. 9 shows the effect of  $r$ -values on the minimum bend radius in such Ti-5Al-2.5Sn alloy sheets respectively. [4] They show that large  $r$ -values are deleterious to the deformations in which the reduction in thickness is mandatory.

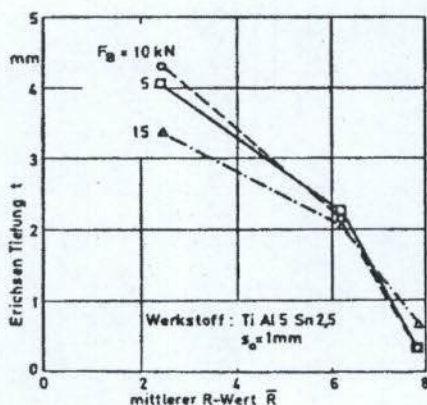


Fig. 8 Effect of  $r$ -values on the Erichsen-value in Ti-5Al-2.5Sn alloy sheets

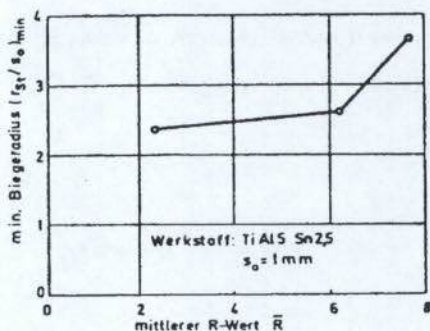


Fig. 9 Effect of  $r$ -values on the minimum bend radius in Ti-5Al-2.5Sn alloy sheets

In conclusion, at this example, the importance of the analysis of the strain condition at bending, of clarifying the relationship between  $r$ -value, texture and bendability, and of clarifying the texture formation mechanism etc. is to be emphasized.

## 2 Development of high strength brass for synchronizer ring

( Application of the characteristics of intermetallic compound to the real product )

Copper alloys are inferior in price competence and strength to steel, so it is seldom that copper alloys are used as structural material. Nevertheless, they are still being used utilizing their wear and corrosion resistant characteristics. An example among them is the synchronizer ring for manual transmission car. Fig. 10 shows the form of the synchronizer ring.

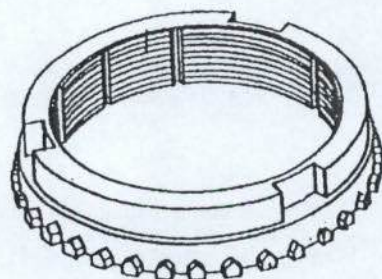


Fig. 10 The form of the synchronizer ring (Diameter about 100mm)



The biggest requirement to synchronizer ring is the wear resistant characteristics. Recent researches show that the following factors are effective in wear resistant characteristics.

- (1) large work hardening
- (2) good thermal conductivity
- (3) good formability of stable oxide film
- (4) existence of appropriate dispersed particles
- (5) good sustainability for dispersion particles (appropriate strength and ductility of the matrix)
- (6) Thermal stability of these properties

Although there are theories in each factor above, copper-base intermetallic compound is probably the best candidate to this purpose. That is  $\beta'$  brass.

In general, conductivity decreases with increasing alloying element concentration, therefore wear resistance is to decrease with increasing alloying element concentration. Here nearly only one exception is the intermetallic compound. Fig. 11 shows the binary phase diagram of Cu-Zn.

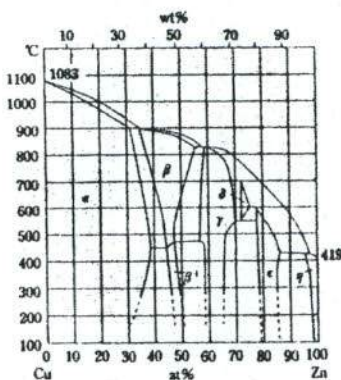


Fig. 11 Cu-Zn binary phase diagram

Although it seems rather complicated, it can be understood as the phase diagram consisting of five peritectic reactions.  $\beta, \gamma, \delta, \epsilon,$  and  $\eta$  intermetallic compounds are formed as result of each peritectic

reaction respectively. Among them,  $\beta$  phase is commercially important. This phase has b.c.c. structure at high temperatures and transforms into the ordered lattice structure under about 450 deg. C. That is the  $\beta'$ -phase. Fig. 12 shows the structures of disordered and ordered b.c.c. structures respectively.

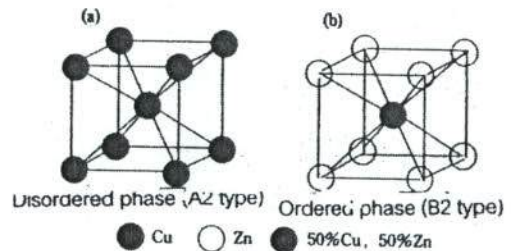


Fig. 12 Structures of disordered and ordered b.c.c. structures of Cu-Zn binary system

In ordered structure, the position of body center is always occupied by another atom and the total atom ratio is 1:1. The ordered structure has limited ductility, therefore it must be worked at high temperatures. Nevertheless, the ordered structure has a big advantage. That is a good conductivity. Since the ordered structure has reduced disorder, electric resistance decreases and conductivity increases. In general, electric resistance increases with increasing alloying elements, therefore intermetallic ordered structure is nearly the only one exception. Good conductivity is beneficial to wear resistance. And it is important to keep the  $\beta \leftrightarrow \beta'$  transition temperature as high as possible. The addition of Al is effective in this meaning. The transition temperature  $\beta \leftrightarrow \beta'$  can be detected clearly by the differential thermal analysis. Fig. 13 shows the schematic structure of Differential Thermal Analysis (DTA). [5]

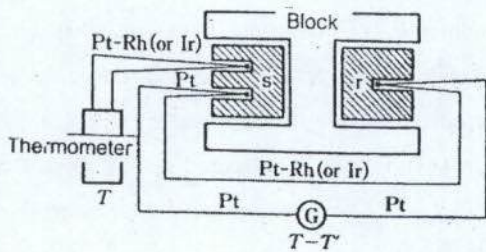


Fig.13 Schematic structure of Differential Thermal Analysis

The relationship between the width of the wear trace in the wear test and  $\beta \leftrightarrow \beta'$  transition temperature is shown in Fig.14.

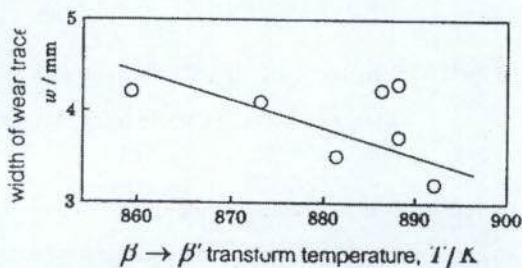


Fig.14 The relationship between the width of the wear trace in the wear test and  $\beta \leftrightarrow \beta'$  transition temperature for various high strength beta brasses

Wear resistance improves with increasing transition temperature. Similar relation is found in the wear of die steel in hot forging. Since the strength of die steel decreases abruptly at the  $A_1$  transition temperature, wear resistance of die steel also improves with increasing transition temperature.[6] In general, wear resistance of material has been evaluated by various wear tests, but wear tests are ways of testing compound characteristics containing many factors. Therefore it is necessary to break down wear resistance into each factor independent to each other. And then the step can be taken to improve it.

In conclusion here, it should be emphasized that the factorization is one of the most important steps in R &D.

### 3 Clarification of corrosion mechanism of Zircaloy for nuclear fuel cladding

(Application of electrochemistry to the real product)

Zr belongs to 4A group in the periodic table and has the similar chemical characteristics with Ti. While Ti is peculiar in density, Zr is peculiar in the small thermal neutron absorption capability. Making use of this property, the Zr alloy, Zircaloy (Zr -1.5% Sn-0.2%Fe-0.15%Cr), is used as the nuclear fuel cladding material in the commercial light water nuclear reactor. Fig. 15 shows the nuclear fuel assembly in which Zircaloy cladding tubes are used.

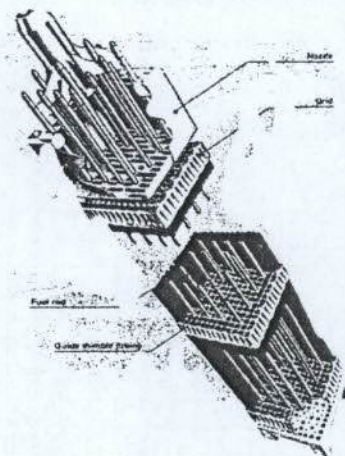


Fig. 15 Nuclear fuel assembly in which Zircaloy cladding tubes are used

Zircaloy nuclear fuel cladding tubes must transfer heat from the fuel inside to water outside and contain radioactive nuclear fission products inside tubes. For that purpose, Zircaloy must resist the corrosion by hot water at about 400 deg. C.



Nearly 50 years have passed since Zircaloy has been developed, but the meaning of the chemical composition has not been known, only it is said that Sn is added for solution strengthening and Fe and Cr are added for corrosion resistance. Recently, it has become clear empirically that the condition of precipitates, especially the size of the precipitates of Zr-Fe-Cr intermetallic compounds, has the significant effect on corrosion resistance of Zircaloy. Furthermore, it has become also clear that the size of precipitates is controlled by the standardized annealing time,

$A = t \exp(-Q/RT)$ , where  $t$  is annealing time,  $Q$  is activation energy,  $R$  is gas constant and  $T$  is annealing temperature. Annealing processes are repeated until the final product, therefore the accumulated annealing parameter is defined as follows:  $\sum A_i = \sum t_i \exp(-Q/RT_i)$

Fig. 16 shows the relationship between the mean size of precipitates and the accumulated annealing time. At the same time, the corrosion rates of these materials in the 350 deg.C pure water corrosion tests are shown in Fig.17.[7]

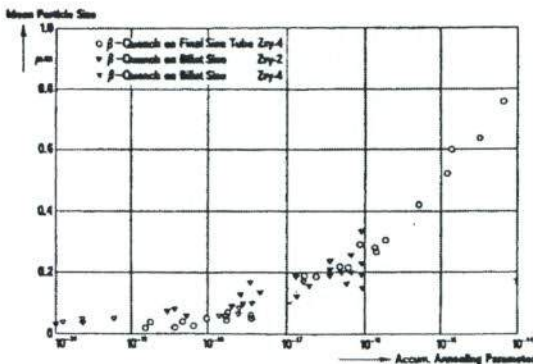


Fig.16 Relationship between the mean size of precipitates and the accumulated annealing time in Zircaloy

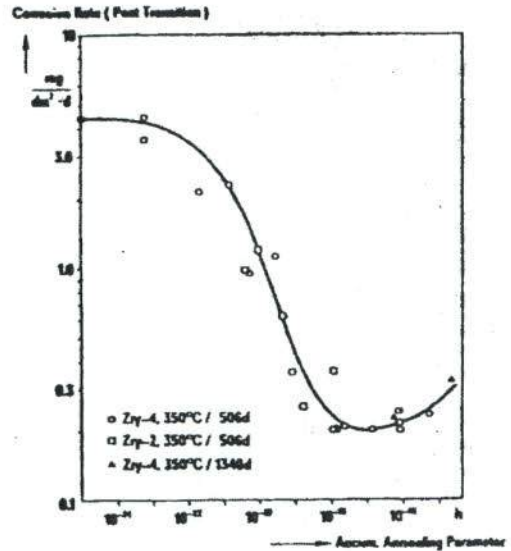


Fig. 17 Corrosion rates of these materials in Fig. 16 in the 350 deg.C pure water corrosion tests

According to these figures, it appears that the size of precipitates begins to increase and the corrosion rate is low when the accumulated annealing time goes over  $10^{-18}h$ , namely it is shown that the size of precipitates should be larger than the critical size to maintain good corrosion resistance.

But they are all empirical rules. Theoretical explanation is needed to make customers be persuaded. For that purpose, following experiments are conducted. First of all it is questionable whether there are precipitates or not, therefore tentative alloys whose Fe and Cr contents straddle the solvus. As is shown in Fig. 18, three levels of content and three levels of quenching temperature are selected.

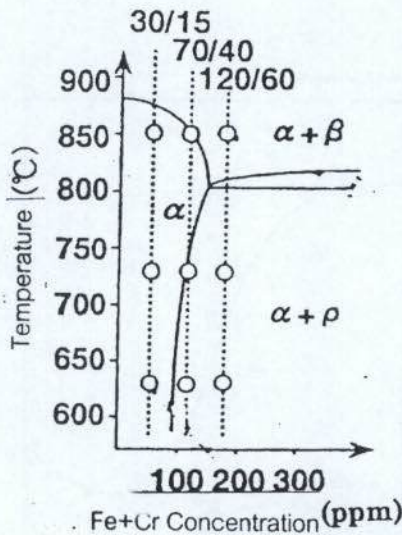


Fig. 18 Fe and Cr contents and quenching temperatures of experimental alloys (Fe content in ppm / Cr content in ppm)

These alloy samples are subjected to corrosion tests and microstructure observations. Fig.19 shows corrosion test results on the phase diagram.

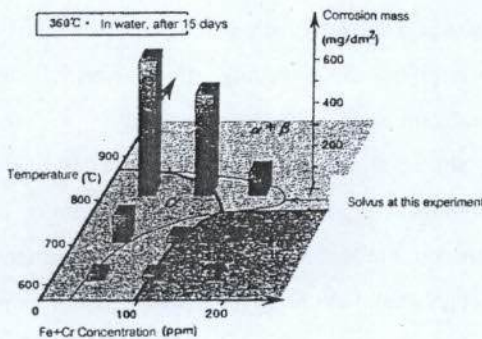


Fig. 19 Corrosion mass of each specimen shown on the phase diagram

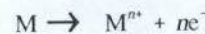
The test results are remarkable, namely, while corrosion masses are extremely large in samples with no precipitates, corrosion masses are small in samples with precipitates.

In general, If something precipitates in the matrix, corrosion resistance degrades, as is typical for Cr carbide precipitation in the austenitic stainless steels. What is the reason why the precipitates improve the corrosion resistance in Zircaloy ? It is suspected due to the anodic protection effect. It is known that in anodic protection the precipitates are noble and enhance the oxidation of the matrix finally leading to passivation, while in cathodic protection the sacrificing anode is less noble and oxidizes protecting matrix.

When the material is corroding in the aqueous solution, the anodic reaction must occur somewhere in the material and at the same time the cathodic reaction must occur elsewhere.

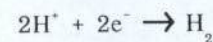
The typical anodic reaction is the oxidation of metal, i.e.:

Anodic Reaction (Oxidation Reaction)



And the typical cathodic reactions are the following two reactions, i.e.:

Cathodic Reaction (Reduction Reaction)



or

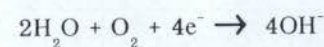


Fig. 20 shows the polarization diagrams.[8]



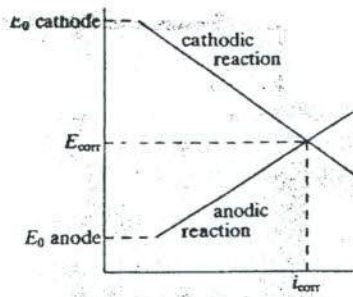


Fig. 20 Anodic and cathodic polarization curves

The potential of anode is lower than that of cathode, but the metal is a conductor, thus potentials must be same. As a result the current flows and the both potentials meet at the new potential, i.e., the corrosion potential. And the current which flows then is the corrosion current. The curve which shows the cathodic reaction is the cathode polarization curve and the one which shows the anodic reaction is the anodic polarization curve.

Then, what is the principle of the anodic protection? Fig.21 is the polarization diagrams which explain the mechanism of the anodic protection.

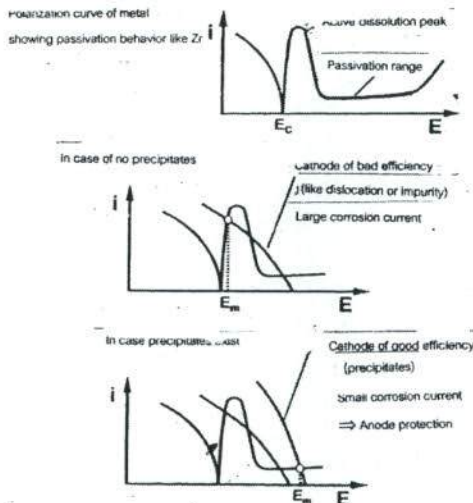


Fig.21 Polarization diagrams which explain the mechanism of the anodic protection

The upper figure shows the cathodic and anodic polarization curves around the natural corrosion potential  $E_c$  of the metal like Zr which shows the passivation behavior. The region where the potential is lower than  $E_c$  is the cathodic reaction region and the region where the potential is higher than  $E_c$  is the anodic reaction region. In metals such as Zr which shows passivation behavior, the anodic polarization curve has the active dissolution region with high corrosion current and the following passivation region with the suppressed corrosion current.

The middle figure shows the corrosion current when the appropriate cathodic points do not exist but only the inappropriate cathodic points such as dislocations and impurities exist. In this case the cathodic polarization curve crosses with the anodic curve of the matrix at the active dissolution range with high corrosion current. Therefore the corrosion resistance is bad.

The bottom figure shows the corrosion current when the appropriate and effective cathodic points do exist. The cathodic polarization curve crosses with the anodic curve of the matrix at the passivation range with low corrosion current. Therefore the corrosion resistance is good. This is the principle of the anodic protection.

From the intuition it can be suspected that the corrosion resistance of Zircaloy is maintained by the anodic protection reaction of precipitates, so the details are studied as follows.

The chemical composition of precipitates in Zircaloy is  $Zr(Cr,Fe)_2$ , where Cr and Fe atoms are interchangeable. In order to separate the effects of Fe and Cr, three kinds of tentative alloys of the chemical compositions of  $ZrFe_2$ ,  $ZrCr_2$  and

$Zr(Cr,Fe)_2$  are produced and polarization curves are measured. Fig. 22 shows the schematic of the electrochemical cells used in this experiment.[9]

CE... Counter Electrode  
WE... Working Electrode  
RE... Reference Electrode  
Li/B... 2.2ppmLi/500ppmB solution  
KCl ... saturated KCl solution

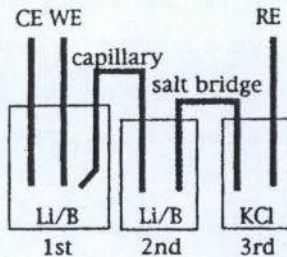


Fig. 22 A schematic of the electrochemical cells

The solution with 2.2 ppm Li and 500 ppm B, made from LiOH and  $H_3BO_3$  reagents and deionized water, was used as the electrolyte. Two electrodes (working and counter) were immersed in the electrolyte in the first cell. The second cell filled with the electrolyte was connected to the first one by the capillary near the working electrode. The third cell, filled with the saturated LCl solution, in which the reference electrode was immersed, was connected to the second cell by a salt bridge of KCl. All cells were set in a water bath controlled at 303 K. Measurements were carried out after deaerating the electrolyte by argon gas. All the working electrodes were held at  $-2000$  mV (versus Ag/AgCl) for 5 min. Then the potentials of the sample was scanned from  $-2000$  mV to  $+2000$  mV at the rate of 20 mV/min. The currents were measured at every 20 s (every 7 mV approximately) and recorded.

Fig. 23 shows the measured polarization curves of each alloy.

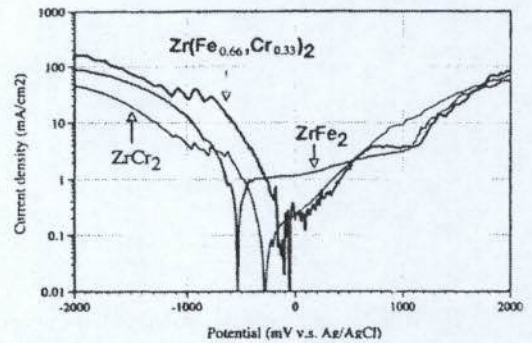


Fig. 23 Measured polarization curves of each alloy which simulates the precipitates in Zircaloy

The left-hand side from the zero-current potential of each alloy is the cathodic polarization curve and the right-hand side is the anodic polarization curve.

According to the cathodic polarization curve of each alloy, the efficiency as the cathode is the best in  $ZrFe_2$  and in  $Zr(Fe,Cr)_2$ , the worst in  $ZrCr_2$ . From this result only, it appears that Cr is not needed for the corrosion resistance of Zircaloy.

But attention must be paid to the anodic polarization curve also. After the Zr matrix is passivated by the anodic protection reaction of precipitates, the precipitates themselves will be corroded. So next the corrosion resistance of precipitates themselves is questioned. Let's focus on the anodic polarization curves. There are some differences between these alloys, i.e., the anodic current is the smallest in  $Zr(Fe,Cr)_2$ , next  $ZrCr_2$ , and the largest in  $ZrFe_2$ . Now the meaning of Cr addition can be understood, i.e., judging from the anodic polarization curves, Cr improves the corrosion resistance of the precipitates and consequently improves the corrosion resistance of Zircaloy. In order to confirm this



suspicion, Zr-0.2% Cr, Zr-0.2%Fe and Zr-0.1%Fe-0.1%Cr alloys are subjected to the corrosion test. Fig. 24 shows the results of the corrosion test. From this practical corrosion test, it is confirmed that the simultaneous addition of Fe and Cr is essential to maintain the good corrosion resistance of Zircaloy.

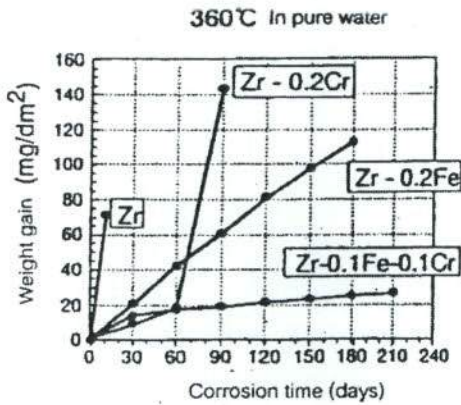


Fig. 24 Corrosion test result of Zr-0.2% Cr, Zr-0.2%Fe and Zr-0.1%Fe-0.1%Cr alloys

In this way, applying the electrochemistry to the precipitates in Zircaloy, the mechanism of corrosion resistance of Zircaloy and the meaning of alloying elements are clarified. Zircaloy has been used more than 40 years, but the mechanism of corrosion resistance has not been known, just only said as a joke that a chunk of stainless steel is added to improve the corrosion resistance of Zr because the stainless steel is corrosion resistant itself. In fact the early Zircaloy contained Ni also. It is often that the material is developed first and the mechanism is clarified later, but the clarification of the mechanism is still important to cope with the accidents and improve the quality still further.

This theory is also useful to think about the corrosion resistance of the weld zone of Zircaloy. After filling

the UO<sub>2</sub> pellets inside the Zircaloy tube, the end of the tube is welded to the Zircaloy plug to seal the tube. This theory teaches the way to select the appropriate welding condition. Welding the plug to the tube is necessary to manufacture the nuclear fuel, therefore we must say that it is lucky that the corrosion resistance is ruled only by the precipitates.

Appendix : The meaning of the standardized annealing time  $A = t_g \exp(-Q/RT)$ .

Fig.16 and 17 in the previous chapter show that the mean particle size and the corrosion rate can be summarized by the standardized annealing time  $A = t_g \exp(-Q/RT)$ . and the accumulated annealing parameter  $\sum A_i = \sum t_i g \exp(-Q/RT_i)$ .

What is the meaning of these two parameters?

In conclusion they mean the diffusion distances Fe and Cr atoms in the Zr-Sn Matrix.

Recently a hypothesis that metallurgical thermal phenomena are ruled by the diffusion distances of the constituent atoms was proposed.[10]

In general, diffusion coefficient  $D$  is expressed by the following equation:

$$D = D_0 \exp(-Q/RT)$$

where  $D_0$  is the frequency factor;  $Q$  is the activation energy of diffusion; and  $R$  is the gas constant.

Next, diffusion distance  $l$  is expressed by the following equation:

$$l = \sqrt{Dt} = \sqrt{D_0} \sqrt{\exp(-Q/RT)}$$

where  $t$  is time.

Namely, the following relationship is obtained between the diffusion distance and the standardized annealing time(SAT).

$$l = C\sqrt{SAT}$$

If the standardized annealing time means the diffusion distance, it is natural that the particle size is summarized by the standardized annealing time(SAT).

#### References

1. C.Newey and G.Weaver: *Materials Principles and Practice*, Butterworth-Heinemann, Oxford, UK, 1990, p.225.
2. A. Tomiura: *Materia*, 37, 1998, p. 3.
3. Y.Mae: *Z. Metallkunde*, 65, 1974, p. 676.
4. Y.Mae; *Industrie Anzeiger*, Vol.23, 10, 1974, p.1963.
5. Y.Saito and M. Kitada, "Roots of Metallurgy", *Uchida Rokakuho*, 2002, p. 234.
6. Y. Tamura: *SOSEI-TO- KAKOU*, No.504, Vol.44, 2003, p. 24.
7. F. Garzarolli et.: *Zirconium in the Nuclear Industry*, 8<sup>th</sup> International Symposium, ASTM STP 1023, ASTM, 1989, p. 202.
8. C.Newey and G.Weaver: *Materials Principles and Practice*, Butterworth-Heinemann, Oxford, UK, 1990, p. 367.
9. T.Murai, T.Isobe, Y. Mae: *J. Nuclear Materials*, 226, 1995, p. 327.
10. Y. Fukuda, Y. Mae et al.: *J. Materials Engineering and Performance*, 11, 2002, p. 544.

#### Author's profile

Enter Mitsubishi Metal mining company (Mitsubishi Materials Corp.) in 1966  
Dr. Eng. from Tokyo University in 1975  
Stay at RTI as a senior volunteer from JICA in 2003

